BIOCHEMISTRY
including biophysical chemistry & molecular biology

Article

pubs.acs.org/biochemistry

Helicobacter pylori TlyA Forms Amyloid-like Aggregates with Potent Cytotoxic Activity

Kusum Lata and Kausik Chattopadhyay*

Centre for Protein Science, Design and Engineering, Department of Biological Sciences, Indian Institute of Science Education and Research Mohali, Sector 81, S. A. S. Nagar, Manauli 140306, Punjab, India

Supporting Information

ABSTRACT: *Helicobacter pylori* is a potent human gastric pathogen. It is known to be associated with several gastroenteric disorders, including gastritis, peptic ulcer, and gastric cancer. The *H. pylori* genome encodes a gene product TlyA that has been shown to display potent membrane damaging properties and cytotoxic activity. On the basis of such properties, TlyA is considered as a potential virulence factor of *H. pylori*. In this study, we show that the *H. pylori* TlyA protein has a strong propensity to convert into the amyloid-like aggregated assemblies, upon exposure to elevated temperatures. Even at the physiological temperature of 37 °C, TlyA shows a strong amyloidogenic property. TlyA aggregates that are generated upon exposure at temperatures of ≥37 °C show prominent binding to dyes like thioflavin T and Nile Red. Transmission electron microscopy also demonstrates the presence of typical amyloid-like fibrils in the TlyA aggregates generated at 37 °C. Conversion of TlyA into the amyloid-like aggregates is found to be associated with major alterations in the secondary and tertiary structural organization of the protein. Finally, our study shows that the preformed amyloid-like aggregates of TlyA are capable of exhibiting potent cytotoxic activities against human gastric adenocarcinoma cells. Altogether, such a propensity of *H. pylori* TlyA to convert into the amyloid-like aggregated assemblies with cytotoxic activity suggests potential implications for the virulence functionality of the protein.

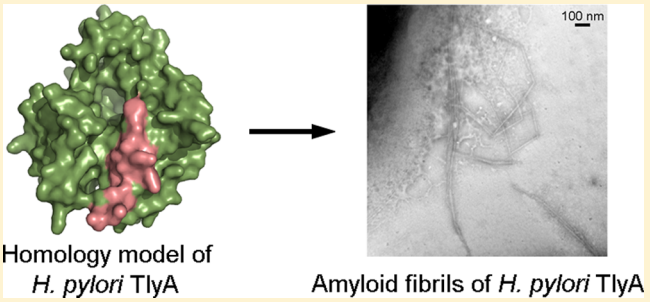

Helicobacter pylori is a Gram-negative bacterial pathogen that causes multiple disorders of the upper gastrointestinal tract in humans.[1,2] Gastric colonization of *H. pylori* has been shown to be associated with diseases such as chronic gastritis, peptic ulcer, and gastric cancer.[3,4] The mechanism of pathogenesis of *H. pylori* employs a number of well-characterized virulence factors, including "cytotoxin-associated gene A" (CagA), proteins encoded in the "*cag*-pathogenicity island", "VacA vacuolating cytotoxin", and urease.[5−8] However, the *H. pylori* genome encodes additional proteins that may potentially contribute to the virulence mechanism of the organism.[9,10]

The *H. pylori* genome encodes a protein (gene product HP1086 in the genome of *H. pylori* strain 26695)[9] that has a sequence similar to that of the TlyA hemolysins of the pathogenic bacteria, like *Serpulina hyodysenteriae*[11] and *Mycobacterium tuberculosis*.[12] Accordingly, the HP1086 gene product has been designated as the TlyA-like protein of *H. pylori*.[13] Recent studies have shown that *H. pylori* TlyA has the potential to contribute to the in vitro hemolytic activity of the organism.[13,14] Mutation in the *tlyA* gene in *H. pylori* compromises the hemolytic activity of the bacteria against erythrocytes.[13] The *tlyA* gene product has also been shown to be associated with the adherence process of *H. pylori* with the host gastric epithelial cells and/or mucosa.[13,15] In its purified form, *H. pylori* TlyA has been shown to display prominent hemolytic activity against human erythrocytes and a potent cytotoxic response against the human gastric adenocarcinoma (AGS) cells.[14] Results obtained from the previous studies indicate that the hemolytic activity of *H. pylori* TlyA arises presumably because of the pore forming activity of the protein in the erythrocyte cell membranes.[14] Membrane damaging activity of TlyA has also been demonstrated against the synthetic lipid vesicles and/or liposomes.[16] The purified form of *H. pylori* TlyA has been found to display potent agglutinating activity and membrane fusion and permeabilization activity against the liposome vesicles.[16] Altogether, it appears that *H. pylori* TlyA exhibits multiple functionalities that are relevant in the context of the *H. pylori* pathogenesis processes.

Although the functionalities of *H. pylori* TlyA have been studied to some extent, a detailed characterization of the physicochemical properties of the protein has not yet been explored. Analysis of the amino acid sequence of *H. pylori* TlyA predicted the presence of region(s) that would make the protein potentially aggregation-prone as well as amyloidogenic. The analysis predicted at least one stretch of sequence (^{148}FISLYYILEAIL^{159}) that has a significant propensity for β-aggregation and amyloid formation (Figure 1). When mapped onto a homology-based structural model of *H. pylori* TlyA, most of the residues within this predicted region were found to

Received: September 25, 2014
Revised: May 21, 2015
Published: May 26, 2015

DOI: 10.1021/acs.biochem.5b00423
Biochemistry 2015, 54, 3649−3659

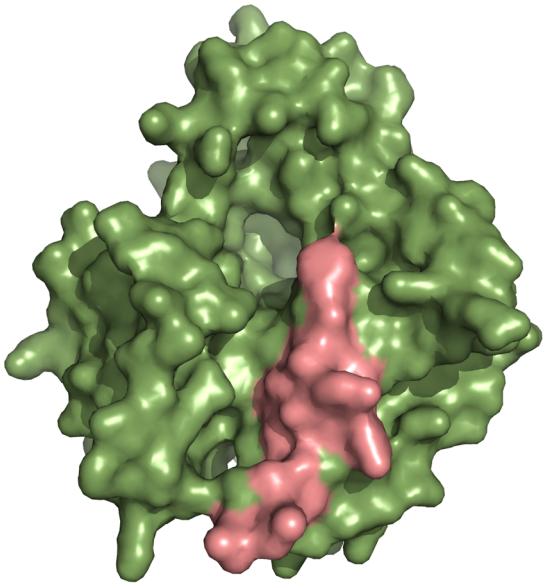

Figure 1. Analysis of the *H. pylori* TlyA amino acid sequence predicts the presence of a region (^{148}FISLYYILEAIL^{159}) that would make the protein potentially aggregation-prone and amyloidogenic. The predicted sequence is highlighted (pale red) in the homology-based structural model of *H. pylori* TlyA (top) and the amino acid sequence of the protein (bottom).

remain exposed on the protein surface (Figure 1). Therefore, in this study, we have explored the possibility of whether the *H. pylori* TlyA protein could display any aggregation and amyloidogenic properties. On the basis of the results of our study, here we report a novel amyloidogenic activity of *H. pylori* TlyA. Our study shows that TlyA has a strong propensity to form aggregates upon being subjected to incubation at temperatures of ≥37 °C. The TlyA aggregates, generated at elevated temperatures of ≥37 °C, show several hallmark features of the amyloid fibrils: (i) enriched with β-sheet secondary structure, (ii) resistance to proteolysis by proteinase K, (iii) binding to dyes like thioflavin T (ThT) and Nile Red, and (iv) formation of aggregated fibril-like structures visible via transmission electron microscopy (TEM). It appears from our data that amyloid-like aggregate formation by TlyA proceeds through a major conformational change(s) that involves opening the exposed hydrophobic patches on the protein surface. Although significant amyloid formation is observed at a physiological temperature of 37 °C, heat treatment to 90 °C could further augment the amyloidogenicity of the protein. Finally, our results show that the preformed TlyA amyloids generated at 37 °C are capable of triggering potent cytotoxic responses in the human AGS cells.

MATERIALS AND METHODS

Protein Purification. The recombinant form of *H. pylori* TlyA was overexpressed and purified following the method described previously[14] with some modifications. Briefly, *Escherichia coli* Origami B cells (Novagen) were transformed with the recombinant pET-14b plasmid harboring the cloned nucleotide sequence encoding *H. pylori* TlyA. *E. coli* cells harboring the recombinant plasmid were inoculated in LB medium (Himedia) supplemented with ampicillin (50 μg/mL) and grown at 37 °C while being constantly shaken. Cells were induced with 0.5 mM isopropyl β-D-thiogalactopyranoside (IPTG) at an OD_{600} of 0.6 were grown for an additional 8 h at 20 °C. Recombinantly generated TlyA with an N-terminal six-His tag was purified from the soluble fraction of the bacterial cell lysate by being passed through the Ni-NTA agarose affinity chromatography resins (Qiagen). His-tagged TlyA bound to the Ni-NTA agarose resins was eluted with PBS [20 mM sodium phosphate and 150 mM NaCl (pH 7.0)] containing 200 mM imidazole. Eluted fractions of the protein were immediately diluted 5-fold with a buffer containing 50 mM sodium phosphate (pH 7.0) and passed through the SP Sepharose cation-exchange resins (Sigma). Bound protein was eluted with 400 mM NaCl in 50 mM sodium phosphate buffer (pH 7.0). The His tag from the TlyA protein was removed by treatment with thrombin as described previously.[14] The presence or absence of the His tag did not affect the properties of the TlyA protein described in this study, to any noticeable extent. Purified protein was analyzed by sodium dodecyl sulfate−polyacrylamide gel electrophoresis (SDS−PAGE) and Coomassie staining. Protein concentrations were estimated either by monitoring the absorbance at 280 nm based on the theoretical extinction coefficient of the protein predicted from the amino acid composition (0.21 for His-tagged TlyA and 0.23 for TlyA without the His tag, at a concentration of 1 mg/mL) or by using the Bradford Reagent (Sigma-Aldrich), with bovine serum albumin as the standard.

Proteinase K Treatment. Structural changes of TlyA upon incubation at various elevated temperatures were monitored by testing the susceptibility of the protein toward proteolytic degradation by proteinase K.[17,18] TlyA (5 μM), in a reaction volume of 100 μL in 50 mM sodium phosphate buffer (pH 7.0), was incubated at various temperatures in the range of 25−100 °C for 15 min. After the treatment, samples were cooled to 25 °C and subjected to proteolysis by using proteinase K, at an enzyme:protein ratio of 1:500 (w/w) for 2 h at 25 °C. Reactions were terminated by boiling the samples for 15 min in the presence of the SDS−PAGE sample buffer containing the reducing agent 2-mercaptoethanol. An equal volume of aliquots from each of the samples was analyzed by SDS−PAGE and Coomassie staining.

Analytical Ultracentrifugation. The solution assembly state of *H. pylori* TlyA at 25 °C was examined by monitoring the sedimentation velocity analytical ultracentrifugation profile on a Beckman Coulter ProteomeLab XL-I analytical ultracentrifuge using an An-50 Ti eight-hole rotor; 380 μL of His-tagged TlyA (absorbance at 280 nm of ∼0.6) in 50 mM sodium phosphate buffer containing 400 mM NaCl (pH 7), and 400 μL of reference buffer was taken in the channels of a two-channel centerpiece (Epon charcoal-filled) with a 12 mm path length and subjected to ultracentrifugation at 42000 rpm and 25 °C. Three hundred absorbance scans were collected for each sample using the continuous scan mode without any time delay between the scans, and the data were analyzed using the continuous $c(S)$ distribution model using SedFit.[19] Partial specific volume (0.752596 mL/g), buffer density (1.02166 g/mL), and viscosity (0.01067 poise) values were calculated using the Sednterp server (http://sednterp.unh.edu/).

DOI: 10.1021/acs.biochem.5b00423
Biochemistry 2015, 54, 3649−3659

Detection of TlyA Oligomers by SDS−PAGE and Coomassie Staining. His-tagged *H. pylori* TlyA protein (5 μM), in a reaction volume of 50 μL in 50 mM sodium phosphate buffer (pH 7.0), was incubated at various temperatures in the range of 25−90 °C for 15 min. After the incubation, samples were brought to 25 °C and treated with SDS−PAGE sample buffer without any reducing agent, and an equal volume of aliquots from each of the samples was subjected to SDS−PAGE and Coomassie staining analysis.

Turbidity Assay for Monitoring Protein Aggregation. Aggregation of *H. pylori* TlyA was monitored by measuring the turbidity of the protein solution.[20] In one experimental setup, His-tagged *H. pylori* TlyA [10 μM, in a reaction volume of 50 μL in 50 mM sodium phosphate buffer (pH 7.0)] was subjected to incubation at various temperatures in the range of 25−100 °C for 15 min. In another setup, TlyA [10 μM, in a reaction volume of 50 μL in 50 mM sodium phosphate buffer (pH 7.0)] was incubated at 37 °C for 15 min to 2 h. We used another experimental strategy in which different concentrations of TlyA [1.25−20 μM, in a reaction volume of 50 μL in 50 mM sodium phosphate buffer (pH 7.0)] were incubated at 37 °C for 15 min. At the end of the incubation, samples were cooled to 25 °C, reaction mixtures were diluted 5-fold with 50 mM sodium phosphate buffer (pH 7.0), and the turbidity of each sample was measured spectrophotometrically at room temperature by recording the OD at 350 nm.

Light Scattering Measurement. The aggregation propensity of TlyA was also monitored by measuring the increase in the light scattering from the protein solution at a right angle with respect to the incident beam. *H. pylori* TlyA (10 μM) in a reaction volume of 2 mL in 50 mM sodium phosphate buffer (pH 7.0) was incubated at a set temperature of either 25 or 37 °C, and light scattering was recorded at 550 nm upon excitation at the same wavelength, using excitation and emission slit widths of 1 nm. Light scattering was measured on a Fluoromax-4 (Horiba Scientific, Edison, NJ) spectrofluorimeter equipped with a Peltier-based temperature controller. Light scattering was recorded at 550 nm, to minimize the contribution of the intrinsic tryptophan fluorescence from the protein samples. Light scattering from the buffer solution without the protein was taken as a control.

Far-UV Circular Dichroism (CD) Spectroscopy. Far-UV CD spectra were recorded on a Chirascan spectropolarimeter (Applied Photophysics, Leatherhead, Surrey, U.K.) equipped with a Peltier-based temperature controller. *H. pylori* TlyA (~2.5 μM) in 1 mM Tris-HCl buffer (pH 8.0) was incubated at a set temperature for a definite period of time, and the far-UV CD spectra were recorded in a quartz cuvette with a 5 mm path length. Four consecutive spectra were recorded, averaged, and buffer subtracted to obtain the final CD spectra of the samples.

Fluorescence Measurements. All the fluorescence measurements were recorded on a Fluoromax-4 (Horiba Scientific, Edison, NJ) spectrofluorimeter equipped with a Peltier-based temperature controller.

ANS (1-anilinonaphthalene-8-sulfonic acid) Fluorescence. All the ANS fluorescence measurements were taken in 50 mM sodium phosphate buffer (pH 7.0), using a final ANS concentration of 10 μM in the solution. Steady state ANS fluorescence was recorded upon excitation at 350 nm, using excitation and emission slit widths of 2 nm. A time-dependent change in the ANS fluorescence was monitored by recording the measurement at 480 nm, upon excitation at 350 nm, using excitation and emission slit widths of 2 nm.

Thioflavin T (ThT) Fluorescence. ThT fluorescence was monitored in 50 mM sodium phosphate buffer (pH 7.0), using a final ThT concentration of 10 μM. ThT fluorescence emission was monitored over 465−550 nm, upon excitation at 450 nm, with excitation and emission slit widths of 2 and 5 nm, respectively.

Nile Red Fluorescence. Nile Red fluorescence emission was measured in 50 mM sodium phosphate buffer (pH 7.0) using a final Nile Red concentration of 2.5 μM, upon excitation at 550 nm with excitation and emission slit widths of 1 and 2 nm, respectively. Nile Red fluorescence emission spectra were recorded over the 575−750 nm wavelength region.

All the fluorescence data are shown after normalization with respect to the maximal fluorescence intensity value in each data set.

Enzyme-Linked Immunosorbent Assay. Binding of native TlyA and binding of the amyloid aggregates of TlyA (generated upon exposure at 37 °C for 30 min) to the Asolectin/cholesterol liposomes were monitored and compared using an enzyme-linked immunosorbent assay (ELISA)-based assay, as described previously.[16,21]

Transmission Electron Microscopy. The structural morphology of the TlyA amyloid fibrils was visualized by transmission electron microscopy (TEM). TlyA (10 μM) in a reaction mixture of 500 μL in PBS was incubated at 37 °C for 4−6 h. Five microliters of the sample was placed on a carbon-coated grid and allowed to incubate for 3 min. After incubation, the excess liquid was absorbed by carefully applying a torn edge of filter paper at the edge of the grid. For staining, a 1% phosphotungstic acid solution was freshly prepared in water. For negative staining of the sample, 5 μL of a 1% phosphotungstic acid solution was immediately applied to the grid and allowed to incubate for 3 min, and after the incubation, excess stain was removed as mentioned above. Samples on the grid were air-dried and immediately analyzed with a Hitachi H7500 transmission electron microscope at the Sophisticated Analytical Instrumentation Facility of Panjab University (Chandigarh, India).

Assay of Cell Viability and Cytotoxicity. Preformed amyloid-like aggregates of TlyA were tested for their ability to trigger cytotoxic responses against the human gastric adenocarcinoma (AGS) cells. The human AGS cell line was obtained from the National Center for Cell Science (NCCS, Pune, India) and maintained in DMEM-F12K medium (Invitrogen) containing 10% fetal bovine serum (FBS, Invitrogen) and a 1% antibiotic and antimycotic solution (Himedia laboratories Pvt. Ltd.) at 37 °C in a 5% CO_2 environment with 95% humidity. For monitoring the cytotoxicity and conducting the cell viability assay, AGS cells (5×10^4 cells per well per 100 μL) were plated in a 96-well plate in phenol red-free DMEM medium (Invitrogen) supplemented with 10% FBS and a 1% antibiotic and antimycotic solution and treated with native TlyA or the preformed amyloid aggregates of the protein (generated by incubation at 37 °C for 4 h) for 24 h at 37 °C. In a separate experimental setup, cells were treated with native TlyA or the preformed amyloids of the protein (corresponding to a total protein concentration of 20 μM) for a defined time period over 6−24 h. Release of lactate dehydrogenase (LDH) in the AGS cell culture medium was estimated as the indicator of cytotoxicity using the CytoTox 96 Non-Radioactive Cytotoxicity Assay Kit (Promega) following the manufacturer's protocol. Maximal LDH release corresponding to the 100%

DOI: 10.1021/acs.biochem.5b00423
Biochemistry 2015, 54, 3649−3659

cytotoxicity was induced by treating the cells with a lysis solution supplied in the kit. AGS cell viability was monitored by the 3-(4,5-dimethylthiazol-2-yl)-2,5-diphenyltetrazolium bromide (MTT)-based assay kit (Sigma-Aldrich) following the manufacturer's protocol. Cells without any treatment were taken for calculating the 100% viability, while the medium blank without any cell represented 0% cell viability.

***In Silico* Analysis of *H. pylori* TlyA.** The amino acid sequence of *H. pylori* TlyA was analyzed for the presence of region(s) that would make the protein potentially aggregation-prone and amyloidogenic. A sequence having β-aggregation propensity was predicted with the TANGO server (http://tango.crg.es/).[22−24] The amyloidogenic sequence was predicted with the WALTZ server (http://waltz.switchlab.org./).[25]

The homology-based structural model of *H. pylori* TlyA was constructed with the SWISS-MODEL server (http://www.expasy.org/spdbv/) using the structural coordinates of Protein Data Bank (PDB) entry 3HP7 as the template, as described previously.[14] The structural model of the protein was visualized with PyMOL.[74]

RESULTS AND DISCUSSION

Exposure of *H. pylori* TlyA to Elevated Temperatures of ≥37 °C Confers Resistance against Proteolytic Degradation by Proteinase K. The proteolysis profile upon treatment with proteinase K is widely used to assess the structural and/or conformational states of the proteins.[18,26,27] Therefore, in characterizing the physicochemical properties of *H. pylori* TlyA, we first monitored its susceptibility to proteinase K digestion. In our assay, TlyA was incubated at a defined temperature in the range of 25−100 °C. Subsequently, it was cooled to room temperature (25 °C) and then subjected to proteolysis with proteinase K. TlyA incubated at 25 °C was found to display profound degradation upon proteinase K treatment (Figure 2). Interestingly, TlyA exposed to elevated temperatures of ≥37 °C exhibited marked resistance toward proteinase K activity (Figure 2); only a marginal extent of proteolytic degradation (in terms of the appearance of the lower-molecular mass bands) was noticed in the case of the TlyA samples exposed to the elevated-temperature conditions. It, therefore, appeared from our data that the exposure of *H. pylori* TlyA to the elevated temperatures allowed the protein to attain a conformation showing resistance against proteinase K-mediated proteolysis.

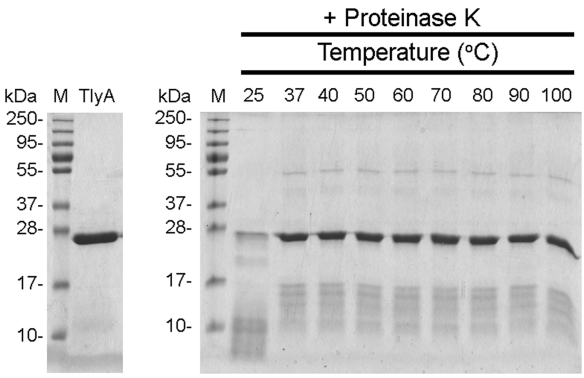

Figure 2. Susceptibility of *H. pylori* TlyA to proteinase K digestion upon exposure to different temperatures in the range of 25−100 °C. Protein samples were incubated at the set temperature for 15 min. Subsequently, the samples were cooled to 25 °C and subjected to the proteinase K treatment for 2 h at 25 °C. Samples were analyzed by SDS−PAGE and Coomassie staining. The right panel shows the proteinase K digestion profile of *H. pylori* TlyA exposed to various temperature conditions as indicated at the top. The left panel shows the TlyA protein without proteinase K treatment as a control. Molecular weight standards are shown as indicated (lane M).

Exposure to an Elevated Temperature of ≥37 °C Triggers Aggregation of *H. pylori* TlyA. Resistance to proteinase K digestion is commonly observed to be associated with aggregation of the proteins in solution. Therefore, we explored the possibility of whether *H. pylori* TlyA could display any aggregation propensity when exposed to an elevated temperatures of ≥37 °C.

The sedimentation velocity analytical ultracentrifugation profile showed that at 25 °C His-tagged TlyA existed mostly as a monomeric species (with a molecular mass of ∼29 kDa) in solution. A small fraction of the protein was found to be present as ∼78 kDa species (Figure 3A). Exposure to elevated temperatures starting from 37 °C for 15 min, however, appeared to trigger formation of SDS-stable, heterogeneous, oligomeric/aggregated species by the TlyA protein, as revealed by the nonreducing SDS−PAGE and Coomassie staining profile (Figure 3B).

To test further the aggregation propensity of *H. pylori* TlyA, the purified form of the protein (10 μM) was subjected to incubation at a temperature in the range of 25−100 °C for 15 min. After the incubation at a defined set temperature, the protein was cooled to 25 °C and then tested for aggregation by monitoring the turbidity of the solution at 350 nm. The TlyA solution kept at 25 °C did not display any noticeable extent of turbidity (Figure 4A). No significant increase in turbidity was observed up to 29 °C. However, exposure to elevated temperatures of ≥31 °C resulted in a gradual increase in the turbidity of the protein solution, thus suggesting temperature-dependent aggregation of TlyA (Figure 4A). Within the temperature range of 29−37 °C, the aggregation propensity was found to increase gradually, with every temperature jump of 2 °C. A more drastic increase in aggregation was noticed, when the incubation temperature was elevated from 37 to 40 °C (Figure 4A). Under the set experimental condition, incubation at 50−60 °C was found to trigger the maximal extent of aggregation. Heat treatment beyond this temperature range did not cause any further significant enhancement of the aggregation of TlyA (Figure 4A).

When the the TlyA solution was incubated at the physiologically relevant temperature of 37 °C, its turbidity was also found to increase in a time- and concentration-dependent manner (Figure 4B,C). When tests were performed at a protein concentration of 10 μM at 37 °C, a steady increase in the turbidity was observed over a period of 0−1 h (Figure 4B). Moreover, when TlyA was incubated at 37 °C for 15 min, an increase in its concentration over the range of 1.25−20 μM was also found to induce gradual enhancement of the turbidity of the protein solution (Figure 4C). Apart from the turbidity assay mentioned above, light scattering measurements also confirmed the aggregation propensity of TlyA at 37 °C. When a solution of TlyA (10 μM) was incubated at 37 °C over a period of 1 h, it showed a steady increase in its light scattering (Figure 4D). In contrast, no significant enhancement of light scattering was observed when the sample was kept at 25 °C (Figure 4D). These data, altogether, suggested a profound aggregation propensity of TlyA, even at a physiological temperature of 37 °C.

DOI: 10.1021/acs.biochem.5b00423
Biochemistry 2015, 54, 3649−3659

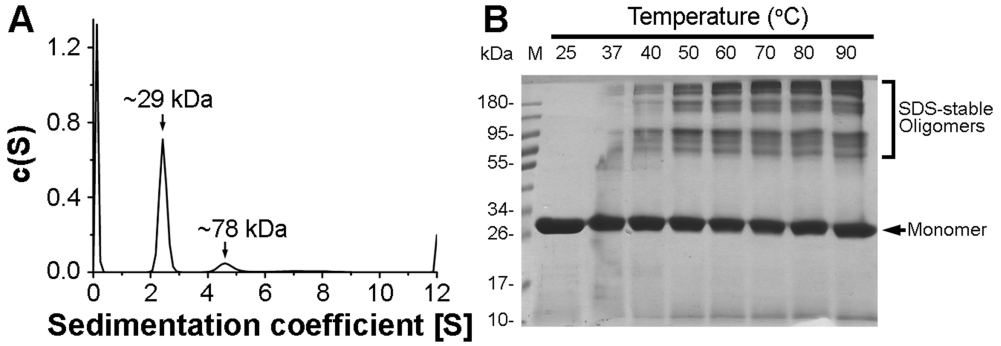

Figure 3. Formation of aggregated oligomers by *H. pylori* TlyA upon exposure to elevated temperatures of ≥37 °C. (A) Sedimentation velocity analytical ultracentrifugation profile of *H. pylori* TlyA at 25 °C. (B) Nonreducing SDS−PAGE and Coomassie staining profile of TlyA upon exposure to different temperature conditions in the range of 25−100 °C. Protein samples were incubated at a set temperature for 15 min. Subsequently, the samples were cooled to 25 °C and analyzed by SDS−PAGE and Coomassie staining under nonreducing conditions. Molecular weight standards are shown as indicated (lane M).

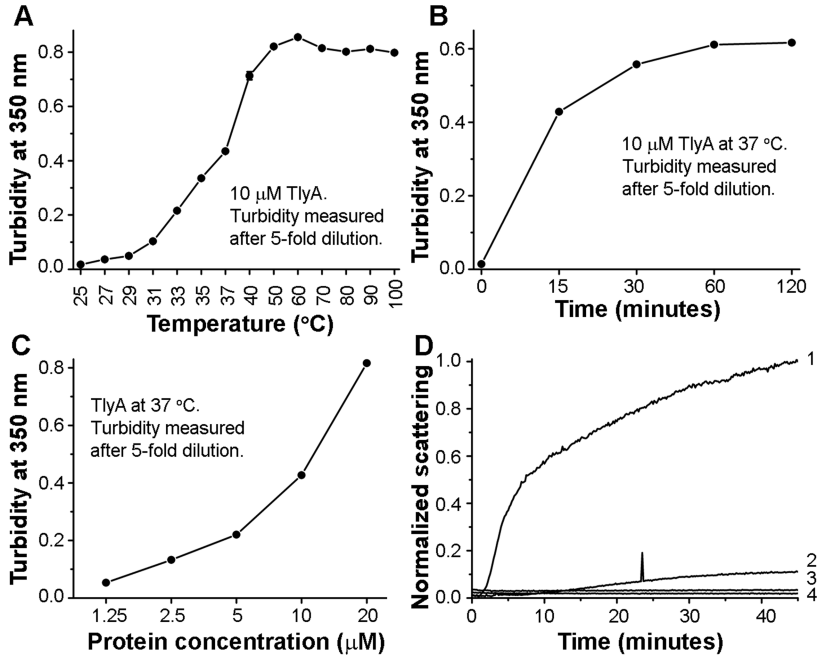

Figure 4. Aggregation of *H. pylori* TlyA upon exposure to elevated temperatures of ≥37 °C. (A) TlyA (10 μM) was incubated at various set temperatures for 15 min. At the end of the incubation, samples were cooled to 25 °C and diluted 5-fold, and the turbidities of the samples were monitored spectrophotometrically by measuring the OD at 350 nm. (B) TlyA (10 μM) was incubated at 37 °C for defined time periods and cooled 25 °C, and the turbidity at 350 nm was recorded after 5-fold dilution. (C) Various concentrations of TlyA were incubated at 37 °C for 15 min and cooled to 25 °C, and the turbidities of the samples at 350 nm were recorded after 5-fold dilution. (D) *H. pylori* TlyA (10 μM) was incubated at either 37 °C (curve 1) or 25 °C (curve 2), and right angle light scattering from the sample solution was monitored spectrofluorimetrically at 550 nm upon excitation at the same wavelength. Light scattering from the buffer solutions kept at 37 °C (curve 3) and 25 °C (curve 4) was recorded as a control.

Incubation of *H. pylori* TlyA at Elevated Temperatures of ≥37 °C Triggers Major Changes in the Secondary and Tertiary Structural Organization of the Protein. In the next part of our study, we wanted to explore whether the heat-induced aggregation of TlyA involved any major structural change(s) in the protein. Because TlyA showed a marked tendency to form aggregates starting from 37 °C, we tested the changes in the secondary and tertiary structural organization of the protein upon incubation at temperatures in the range of 37−90 °C.

Incubation of H. pylori TlyA at ≥37 °C Triggers a Conformational Change toward Enriched β-Secondary Structures. As reported previously,[14] far-UV CD spectra of TlyA at 25 °C showed a broad spectrum of negative ellipticity between the wavelengths of 208 and 222 nm, with the negative ellipticity value peaking at around 208 nm. Interestingly, exposure of TlyA for 15 min at an elevated temperatures of ≥37 °C (up to 85 °C; at an interval of 12 °C) resulted in a considerable change in the far-UV CD profile of the protein (Figure 5A). Starting from an incubation temperature of 37 °C, the spectra appeared to become more symmetric, and the peak of negative ellipticity minimum approached 218 nm (Figure 5A). Such a change in the far-UV CD profile of TlyA could be interpreted as the structural/conformational transition of the protein toward a state having enriched β-secondary structures. It is important to mention here that the secondary structural change in TlyA, induced upon exposure at 37 °C for 15 min, was not augmented further during prolonged incubation for up

DOI: 10.1021/acs.biochem.5b00423
Biochemistry 2015, 54, 3649−3659

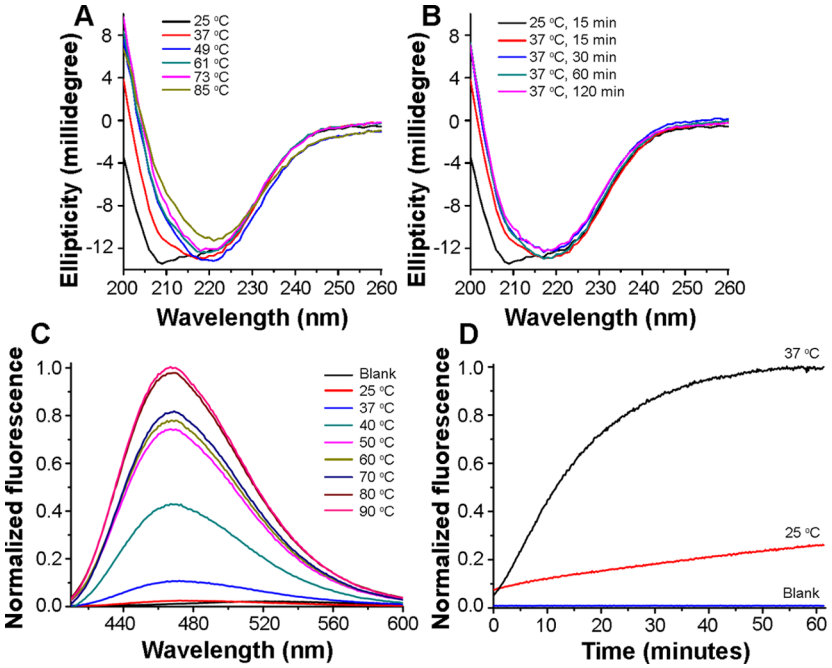

Figure 5. Changes in the secondary and tertiary structural organization of *H. pylori* TlyA upon exposure to elevated temperatures of ≥37 °C. (A) Far-UV CD spectra of TlyA after incubation at various set temperatures for 15 min. (B) Far-UV CD spectra of TlyA upon incubation at 37 °C for various time periods. (C) ANS fluorescence at 25 °C in the presence of TlyA upon exposure of the protein to various set temperatures for 15 min. All the ANS fluorescence spectra were corrected by subtracting those of the protein samples in the absence of ANS. ANS fluorescence in the absence of TlyA served as the blank. (D) Time-dependent change in the ANS fluorescence in the presence of TlyA at 37 °C (black) and 25 °C (red). ANS fluorescence at 25 °C in the absence of TlyA served as the blank (blue).

to 2 h (Figure 5B). Rather, incubation for 15 min at further elevated temperatures in the range of 49−85 °C caused a more profound change in the secondary structural organization of TlyA, as observed in terms of the shift in the negative ellipticity minima toward the wavelength region of 219−221 nm (Figure 5A).

Incubation of H. pylori TlyA at Elevated Temperatures of ≥37 °C Induces Changes in the Tertiary Structural Organization in Terms of Opening the Exposed Hydrophobic Patches on the Protein Surface. We wanted to explore whether the exposure to elevated temperatures resulted in any global tertiary structural change in TlyA. For this, we tested the ability of TlyA to bind to ANS (1-anilinonaphthalene-8-sulfonic acid), upon exposure at elevated temperatures of ≥37 °C. ANS is a hydrophobic dye having environment-sensitive fluorescence properties.[28,29] ANS is nonfluorescent in aqueous environment but shows significantly enhanced fluorescence along with dramatic blue shift in the fluorescence emission maxima when placed in a nonpolar and hydrophobic environment. Consistent with a such property, binding of ANS to surface-exposed hydrophobic patches present on the partially folded/unfolded states of proteins triggers increased fluorescence emission, along with a blue shift in the emission maxima. In contrast, no such change in the ANS fluorescence is generally observed in the presence of proteins having a native folded state, or those in their fully denatured state, as such conformations do not display any prominent surface-exposed hydrophobic patch.[29−32] On the basis of such observations, the ANS binding propensity has been widely used to characterize global tertiary structural alternations in the proteins.[33−35]

To test ANS binding, a TlyA concentration of 10 μM was incubated at a set temperature in the range of 25−90 °C for 15 min. After the incubation, protein was cooled to 25 °C, ANS was added to the protein sample, and ANS fluorescence emission was recorded upon excitation at 350 nm. It was observed that ANS fluorescence in the presence of TlyA incubated at 25 °C was almost insignificant, while ANS fluorescence emission increased steadily when monitored in the presence of TlyA exposed to the increasing elevated temperature conditions (Figure 5C). Consistent with its binding to the exposed hydrophobic patches on the protein surface,[36−38] ANS fluorescence emission maxima in the presence of TlyA were observed in the region at ∼470 nm. These data suggested that the exposure of TlyA at elevated temperatures of ≥37 °C resulted in the formation of exposed hydrophobic patches on the surface of the protein. The results further implied prominent change(s) in the global tertiary structural organization of TlyA when it was subjected to treatments at elevated temperatures.

It is important to note that TlyA, even when exposed to the physiological temperature of 37 °C for 15 min, showed significant ANS binding in terms of triggering increased ANS fluorescence emission (Figure 5C and Figure S1 of the Supporting Information). At a concentration as low as 1.25 μM, TlyA also showed a detectable extent of ANS binding (Figure S1A of the Supporting Information). To gain more insight into the ANS binding propensity of TlyA at 37 °C, we monitored the kinetics of ANS fluorescence in the presence of TlyA (10 μM) at 37 °C and compared the measured kinetics to that at 25 °C. In this experimental setup, ANS was added to the protein sample, and subsequently, the ANS fluorescence (at 480 nm upon excitation at 350 nm) was recorded while the sample was incubated at a set temperature of either 37 or 25 °C, over a period of 1 h. We observed a steady increase in the ANS fluorescence in the presence of TlyA at 37 °C, while incubation in the presence of TlyA at 25 °C resulted in a

DOI: 10.1021/acs.biochem.5b00423
Biochemistry 2015, 54, 3649−3659

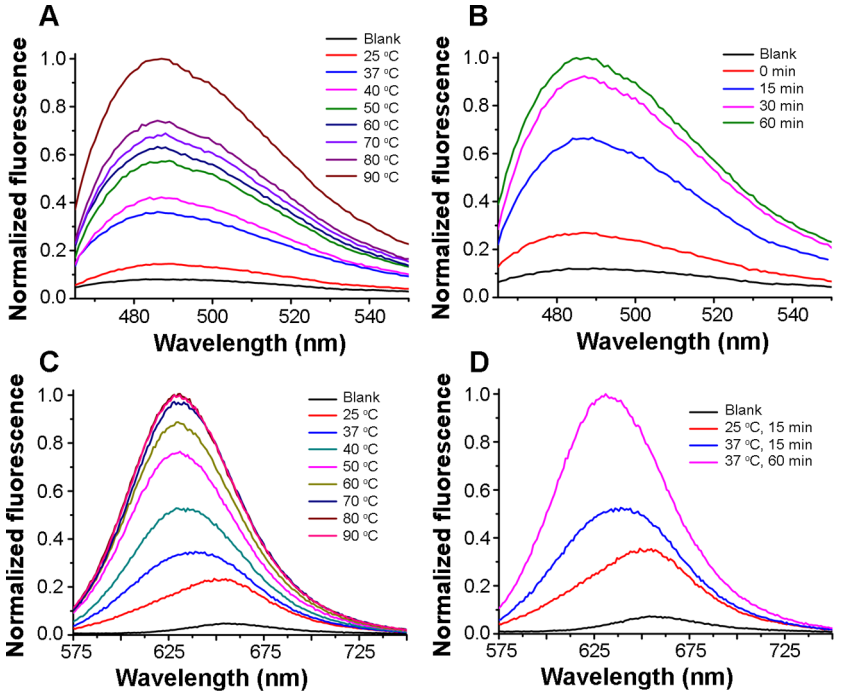

Figure 6. Amyloidogenicity of *H. pylori* TlyA upon exposure to elevated temperatures of ≥37 °C. (A) ThT fluorescence at 25 °C in the presence of TlyA upon exposure of the protein to various set temperatures for 15 min. All the ThT fluorescence spectra were corrected by subtracting those of the protein samples in the absence of ThT. ThT fluorescence in the absence of TlyA served as the blank. (B) ThT fluorescence at 25 °C in the presence of TlyA upon incubation of the protein at 37 °C for various time periods. All the ThT fluorescence spectra were corrected by subtracting those of the protein samples in the absence of ThT. ThT fluorescence in the absence of TlyA served as the blank. (C) Nile Red fluorescence at 25 °C in the presence of TlyA upon exposure of the protein to various set temperatures for 15 min. All the Nile Red fluorescence spectra were corrected by subtracting with those of the protein samples in the absence of Nile Red. Nile Red fluorescence in the absence of TlyA served as the blank. (D) Nile red fluorescence at 25 °C in the presence of TlyA upon incubation of the protein at 37 °C for various time points. All the Nile Red fluorescence spectra were corrected by subtracting those of the protein samples in the absence of Nile Red. Nile Red fluorescence in the absence of TlyA served as the blank.

marginal increase in the ANS fluorescence intensity (Figure 5D). ANS fluorescence in the presence of TlyA at 37 °C was found to approach saturation after incubation for ∼40 min. These results clearly showed that the exposure of TlyA even at 37 °C triggered a sufficient extent of ANS binding, thus suggesting prominent tertiary structural change(s) in the protein in terms of opening of surface-exposed hydrophobic patches. Such a structural/conformational change may have acted as the triggering factor for the aggregation property of TlyA observed at the elevated-temperature conditions. Notably, an increased number of surface-exposed hydrophobic patches on TlyA, triggered at elevated temperatures, did not alter the ability of the protein to associate with the membrane lipid bilayer. As described in a previous study, native TlyA shows strong binding to the membrane lipid bilayer of synthetic lipid vesicles and/or liposomes.[16] In the same vein, we tested and compared the binding of the native TlyA protein and the TlyA aggregates (generated upon exposure at 37 °C for 30 min) to the Asolectin/cholesterol liposomes. The results obtained from the ELISA-based binding assay revealed that both variants of TlyA showed similar extents of binding to the Asolectin/cholesterol liposomes, when tested over the protein concentration range 0.3125−5 μM (Figure S1B of the Supporting Information).

Exposure of *H. pylori* TlyA at Elevated Temperatures of ≥37 °C Triggers Conversion of the Protein into the Amyloid-like Structures. Analysis of the *H. pylori* TlyA primary structure predicted the presence of sequence motif(s) that would make the protein potentially aggregation-prone and amyloidogenic (Figure 1). Consistent with such a prediction, our data showed a potent aggregation propensity of *H. pylori* TlyA when it was subjected to the elevated temperatures starting from the physiological temperature of 37 °C. In the next part of our study, we explored the possibility of whether TlyA could exhibit any tendency to form amyloid-like structures upon exposure to the elevated temperatures. For this, we monitored the binding of amyloid-specific dyes like ThT (thioflavin T) and Nile Red with TlyA. We also examined the formation of amyloid fibrils by using transmission electron microscopy (TEM).

ThT Fluorescence Assay. ThT, in general, does not interact with the proteins in their native, molten globule, and unfolded states, and it does not bind to the amorphous aggregates of the proteins either. ThT shows specific association with the protein amyloids and amyloid-like fibrils; upon such specific interaction, ThT becomes highly fluorescent.[29,39−43] On the basis of such properties, ThT fluorescence is widely used to monitor amyloid formation.[44−47] To test any possible amyloidogenic property of *H. pylori* TlyA, we monitored ThT fluorescence in the presence of the protein upon exposure to various temperatures in the range of 25−90 °C. In our experimental setup, TlyA (at a concentration of 20 μM) was incubated at a defined temperature for 15 min. After the incubation, protein was cooled to 25 °C, ThT was added to the sample, and ThT fluorescence was monitored upon excitation at 450 nm. TlyA incubated at 25 °C did not show any

DOI: 10.1021/acs.biochem.5b00423
Biochemistry 2015, 54, 3649−3659

significant ThT fluorescence, while exposure of the protein to elevated temperatures of ≥37 °C (up to 90 °C) induced a steady increase in ThT fluorescence emission (Figure 6A). In another experimental setup, where TlyA (20 μM) was exposed to a physiological temperature of 37 °C for a prolonged duration of up to 60 min, it also induced a time-dependent increase in ThT fluorescence (Figure 6B). Also, at a lower protein concentration range of ≤2.5 μM, TlyA induced prominent ThT fluorescence at 37 °C, upon being incubated for a period of 15 min (Figure S2A of the Supporting Information). These results suggested that the exposure of TlyA to elevated temperatures of ≥37 °C triggered conversion of the protein to amyloid-like structures capable of showing prominent ThT binding. Even at 37 °C, TlyA appeared to form amyloid-like structures to a considerable extent.

Nile Red Fluorescence Assay. We also confirmed the amyloidogenic potential of TlyA by testing its ability to bind to Nile Red, which is also being widely used to probe amyloid fibril formation.[48−50] Nile Red is a hydrophobic dye showing environment-sensitive fluorescence properties. In an aqueous environment, Nile Red exhibits weak solvent-quenched fluorescence in the red wavelength region, and upon being transferred into hydrophobic environments, it shows blue-shifted, enhanced fluorescence emission.[51] Because of such environment-sensitive fluorescence properties, Nile Red binding is commonly observed with diverse amyloid fibrils.[52] In the absence of TlyA, Nile Red showed poor fluorescence emission at ∼655 nm upon excitation at 550 nm. In the presence of TlyA (10 μM) incubated at 25 °C, we observed a marginal increase in Nile Red fluorescence with no prominent shift in the emission maxima (Figure 6C). In contrast, when TlyA was exposed to an elevated temperature in the range of 37−90 °C for 15 min and then cooled to 25 °C, the protein triggered a substantial increase in Nile Red fluorescence, with a prominent blue-shift in the emission maxima toward 625 nm (Figure 6C). With a gradual increase in the incubation temperature to 90 °C, there was a steady enhancement of the Nile Red fluorescence. Even exposure of TlyA at the physiological temperature of 37 °C for 15 min induced a significant increase in Nile Red fluorescence, as compared to that observed at 25 °C (Figure 6C). When TlyA was monitored over a prolonged duration of ≤1 h, its incubation (10 μM) at 37 °C also resulted in a time-dependent increase in Nile Red fluorescence (Figure 6D). At an even lower concentration of 5 μM, TlyA exhibited a noticeable extent of Nile Red binding (Figure S2B of the Supporting Information). Altogether, these results provided further support for the amyloidogenic property of TlyA, upon exposure to elevated temperatures of ≥37 °C.

Transmission Electron Microscopy of the Amyloid Fibrils of TlyA Formed at 37 °C. On the basis of the ThT and Nile Red fluorescence-based assays, it was evident that *H. pylori* TlyA showed a prominent amyloidogenic property, upon being subjected to exposure under the elevated-temperature conditions, including that at the physiological temperature of 37 °C. In the next part of our study, we analyzed the structural morphology of the TlyA amyloids generated at 37 °C by employing transmission electron microscopy (TEM). Traditionally, TEM has been used extensively to characterize the amyloid fibrils.[53−56] Consistent with the typical TEM profile of the amyloid fibrils, the TEM image showed the presence of fibril-like assemblies in the TlyA sample incubated at 37 °C for 4 h (Figure 7). Qualitative analysis of the TEM images showed the presence of fibril-like structures that were ∼200−1000 nm

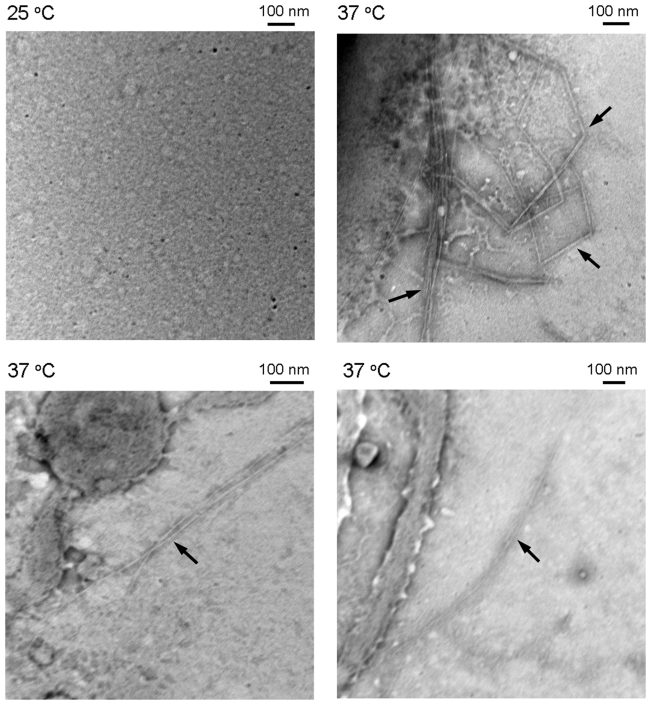

Figure 7. TEM images of the TlyA amyloid fibrils generated by incubation of the protein at 37 °C for 4 h. The TEM image of the TlyA sample at 25 °C did not show any amyloid fibril. Amyloid fibril structures are denoted with arrows.

in length, with the widths of ∼10 nm. In contrast, the TlyA sample kept at 25 °C did not show the presence of any such amyloid fibril-like structures (Figure 7). These results, once again, confirmed formation of the typical amyloid fibrils by TlyA when it was subjected to incubation even at the physiological temperature of 37 °C.

Amyloid Aggregates of TlyA Formed at 37 °C Trigger Cytotoxicity in Human AGS Cells. It has been shown previously that *H. pylori* TlyA exhibits potent cytotoxic activities against human gastric adenocarcinoma (AGS) cells.[14] In such an assay of cytotoxicity, human AGS cells have been treated with TlyA at 37 °C for 24 h, and then the cells have been tested for viability and cytotoxicity. The data obtained in this study show that the prolonged incubation of *H. pylori* TlyA at 37 °C triggered conversion of the protein into the amyloid-like aggregates. Therefore, we wanted to explore whether the preformed amyloid-like aggregates of TlyA, generated at 37 °C, could also exert cytotoxic responses against the human AGS cells. For this, *H. pylori* TlyA protein (at a stock concentration of 80 μM) was incubated at 37 °C for 4 h to allow its conversion into the amyloid-like aggregates. It was found that such treatment allowed complete conversion of TlyA into insoluble aggregates (Figure S3 of the Supporting Information). Subsequently, human AGS cells were treated with the preformed amyloid aggregates of TlyA thus generated and were incubated for a further 24 h at 37 °C. Cytotoxic effects of TlyA amyloids on the human AGS cells were monitored by the LDH-release assay and the MTT-based cell viability assay. Both the LDH-release assay and the MTT assay showed that the preformed TlyA amyloids, generated at 37 °C, induced prominent cytotoxicity against the human AGS cells in a concentration-dependent manner (Figure 8A,B). As observed in the LDH-release assay, preformed TlyA amyloids at a concentration of 20 μM (equivalent to the total TlyA protein

DOI: 10.1021/acs.biochem.5b00423
Biochemistry 2015, 54, 3649−3659

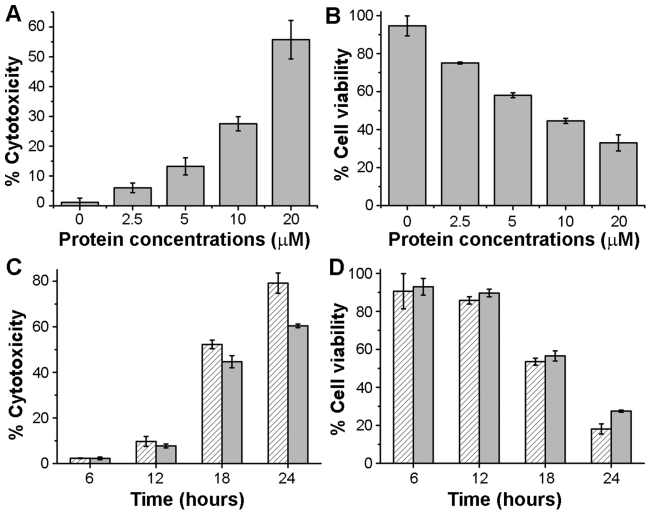

Figure 8. Cytotoxicity of amyloid aggregates of *H. pylori* TlyA against human AGS cells. Amyloid aggregates of TlyA were generated by incubation of the protein at 37 °C for 4 h. (A) Concentration-dependent cytotoxic activity of the TlyA amyloid aggregates against the AGS cells monitored by the LDH-release assay. (B) AGS cell viability upon treatment with various concentrations of TlyA amyloid aggregates estimated by the MTT-based assay. (C) Time course of the cytotoxic activities of native TlyA (shaded bars) and preformed amyloid aggregates of TlyA (hatched bars) against the AGS cells monitored by the LDH-release assay. Protein concentrations were 20 μM. (D) Time course of AGS cell viability upon treatment with the native TlyA (shaded bars) and preformed amyloid aggregates of TlyA (hatched bars) monitored by the MTT-based assay. Protein concentrations of 20 μM were used. Data shown here are the average ± standard deviations of three independent measurements.

concentration) exerted ~55% cytotoxicity in the AGS cells (Figure 8A). Consistent with this, the MTT-based assay also showed a nearly 60% decrease in the viability of the AGS cells, upon treatment with the TlyA amyloids, corresponding to a total protein concentration of 20 μM (Figure 8B). We also compared the time course of the cytotoxicity of the preformed TlyA amyloids with that of the native TlyA protein (Figure 8C,D). In both cases, prominent cytotoxicity was observed only after treatment for 18 h. It is important to note here that the preformed TlyA amyloids showed only marginally increased cytotoxic responses as compared to those triggered by the native TlyA sample, when examined at the 24 h time point (Figure 8C,D). Regardless, altogether these data suggested that the aggregated amyloid-like assemblies of TlyA generated at the physiological temperature of 37 °C exhibited potent cytotoxic activity against human AGS cells.

CONCLUSION

Amyloid aggregates and fibrils represent unique quaternary structural assembly of the proteins, and they are associated with diverse biological processes.[57−61] Formation of amyloid fibrils is typically implicated in the pathogenesis processes associated with various neurodegenerative disorders.[58,62−64] However, amyloids have also been shown to be associated with critical biological functions in diverse organisms such as bacteria, fungi, insects, and humans.[65,66] One of the best studied examples of such, so-called "functional amyloids" of bacterial origin is the Curli.[67,68] Amyloid fibril formation by Curli is implicated in bacterial biofilm formation as well as in the process of host cell adhesion.[68,69] Several bacterial protein toxins are also known to form amyloid-like assemblies,[70] for example, listeriolysin O, a cholesterol-dependent membrane-damaging cytotoxin produced by *Listeria monocytogenes*,[71] TasA from *Bacillus subtilis*,[72] and thermostable direct hemolysin from *Vibrio parahemolyticus*.[73] However, the physiological implications of amyloid formation by these bacterial protein toxins have not been clearly elucidated.

TlyA has been characterized as a potential virulence factor of the human gastric pathogen *H. pylori*.[13,14,16] In this study, we have demonstrated the novel amyloidogenic property of *H. pylori* TlyA. When exposed to an elevated temperature starting from the physiological condition of 37 °C, TlyA shows a prominent tendency to convert into aggregates with classical signatures of the amyloid-like assemblies. Such amyloid formation appears to involve gross secondary and tertiary structural changes in the protein, in terms of acquiring enriched β-secondary structures and opening the surface-exposed hydrophobic patches, respectively. Amyloid-like aggregates of TlyA, generated even at the physiological temperature of 37 °C, display potent cytotoxic responses against human AGS cells, thus representing the functional amyloid forms of the protein. On the basis of the results obtained in this study, it is possible to speculate that such a amyloidogenic property of *H. pylori* TlyA may potentially contribute to the virulence properties of the protein. However, more studies will be required to elucidate the mechanism of amyloid formation by *H. pylori* TlyA. Also, the implications of such an amyloidogenic potential of TlyA in the context of the pathophysiological responses generated during the *H. pylori* infection need to be explored in the future.

ASSOCIATED CONTENT

Supporting Information

ANS binding in the lower protein concentration range of TlyA, upon exposure of the protein to 37 °C for 15 min (Figure S1A), binding of native TlyA and that of the TlyA aggregates (generated upon exposure at 37 °C for 30 min) to the Asolectin/cholesterol liposomes (Figure S1B), ThT binding in the lower protein concentration range of TlyA, upon exposure of the protein to 37 °C for 15 min (Figure S2A), Nile Red binding in the lower protein concentration range of TlyA, upon exposure of the protein to 37 °C for 15 min (Figure S2B), and complete conversion of TlyA into insoluble aggregates upon exposure to 37 °C for 4 h (Figure S3). The Supporting Information is available free of charge on the ACS Publications website at DOI: 10.1021/acs.biochem.5b00423.

AUTHOR INFORMATION

Corresponding Author

*Centre for Protein Science, Design and Engineering, Department of Biological Sciences, Indian Institute of Science Education and Research Mohali, Sector 81, S. A. S. Nagar, Manauli 140306, Punjab, India. Phone: 91-0172-2293147. Fax: 91-0172-2240124. E-mail: kausik@iisermohali.ac.in.

Funding

This work was supported by funding from the Indian Institute of Science Education and Research Mohali (to K.C.), funding under the Centre of Excellence (COE) in Frontier Areas of Science and Technology (FAST) program of the Ministry of Human Resource Development, Government of India, in the area of protein science, design, and engineering (to K.C.), and a Senior Research Fellowship of the Council of Scientific and Industrial research, India (to K.L.).

DOI: 10.1021/acs.biochem.5b00423
Biochemistry 2015, 54, 3649−3659

Notes

The authors declare no competing financial interest.

■ ACKNOWLEDGMENTS

We acknowledge the Sophisticated Analytical Instrumentation Facility of Panjab University for assistance with the transmission electron microscopy study. We thank Ms. Nidhi Kundu of IISER Mohali for her assistance with the analytical ultracentrifugation experiment.

■ ABBREVIATIONS

AGS, gastric adenocarcinoma; ThT, thioflavin T; TEM, transmission electron microscopy; ANS, 1-anilinonaphthalene-8-sulfonic acid.

■ REFERENCES

(1) Kusters, J. G., van Vliet, A. H., and Kuipers, E. J. (2006) Pathogenesis of *Helicobacter pylori* infection. *Clin. Microbiol. Rev. 19*, 449−490.

(2) Montecucco, C., and Rappuoli, R. (2001) Living dangerously: How *Helicobacter pylori* survives in the human stomach. *Nat. Rev. Mol. Cell Biol. 2*, 457−466.

(3) Salama, N. R., Hartung, M. L., and Muller, A. (2013) Life in the human stomach: Persistence strategies of the bacterial pathogen *Helicobacter pylori*. *Nat. Rev. Microbiol. 11*, 385−399.

(4) De Luca, A., and Iaquinto, G. (2004) *Helicobacter pylori* and gastric diseases: A dangerous association. *Cancer Lett. 213*, 1−10.

(5) Argent, R. H., Thomas, R. J., Letley, D. P., Rittig, M. G., Hardie, K. R., and Atherton, J. C. (2008) Functional association between the *Helicobacter pylori* virulence factors VacA and CagA. *J. Med. Microbiol. 57*, 145−150.

(6) Cover, T. L., and Blanke, S. R. (2005) *Helicobacter pylori* VacA, a paradigm for toxin multifunctionality. *Nat. Rev. Microbiol. 3*, 320−332.

(7) Noto, J. M., and Peek, R. M., Jr. (2012) The *Helicobacter pylori* cag Pathogenicity Island. *Methods Mol. Biol. 921*, 41−50.

(8) van Vliet, A. H., Kuipers, E. J., Waidner, B., Davies, B. J., de Vries, N., Penn, C. W., Vandenbroucke-Grauls, C. M., Kist, M., Bereswill, S., and Kusters, J. G. (2001) Nickel-responsive induction of urease expression in *Helicobacter pylori* is mediated at the transcriptional level. *Infect. Immun. 69*, 4891−4897.

(9) Tomb, J. F., White, O., Kerlavage, A. R., Clayton, R. A., Sutton, G. G., Fleischmann, R. D., Ketchum, K. A., Klenk, H. P., Gill, S., Dougherty, B. A., Nelson, K., Quackenbush, J., Zhou, L., Kirkness, E. F., Peterson, S., Loftus, B., Richardson, D., Dodson, R., Khalak, H. G., Glodek, A., McKenney, K., Fitzegerald, L. M., Lee, N., Adams, M. D., Hickey, E. K., Berg, D. E., Gocayne, J. D., Utterback, T. R., Peterson, J. D., Kelley, J. M., Cotton, M. D., Weidman, J. M., Fujii, C., Bowman, C., Watthey, L., Wallin, E., Hayes, W. S., Borodovsky, M., Karp, P. D., Smith, H. O., Fraser, C. M., and Venter, J. C. (1997) The complete genome sequence of the gastric pathogen *Helicobacter pylori*. *Nature 388*, 539−547.

(10) Alm, R. A., Ling, L. S., Moir, D. T., King, B. L., Brown, E. D., Doig, P. C., Smith, D. R., Noonan, B., Guild, B. C., deJonge, B. L., Carmel, G., Tummino, P. J., Caruso, A., Uria-Nickelsen, M., Mills, D. M., Ives, C., Gibson, R., Merberg, D., Mills, S. D., Jiang, Q., Taylor, D. E., Vovis, G. F., and Trust, T. J. (1999) Genomic-sequence comparison of two unrelated isolates of the human gastric pathogen *Helicobacter pylori*. *Nature 397*, 176−180.

(11) Muir, S., Koopman, M. B., Libby, S. J., Joens, L. A., Heffron, F., and Kusters, J. G. (1992) Cloning and expression of a *Serpula* (*Treponema*) *hyodysenteriae* hemolysin gene. *Infect. Immun. 60*, 529−535.

(12) Wren, B. W., Stabler, R. A., Das, S. S., Butcher, P. D., Mangan, J. A., Clarke, J. D., Casali, N., Parish, T., and Stoker, N. G. (1998) Characterization of a haemolysin from *Mycobacterium tuberculosis* with homology to a virulence factor of *Serpulina hyodysenteriae*. *Microbiology 144* (Part 5), 1205−1211.

(13) Martino, M. C., Stabler, R. A., Zhang, Z. W., Farthing, M. J., Wren, B. W., and Dorrell, N. (2001) *Helicobacter pylori* pore-forming cytolysin orthologue TlyA possesses in vitro hemolytic activity and has a role in colonization of the gastric mucosa. *Infect. Immun. 69*, 1697−1703.

(14) Lata, K., Paul, K., and Chattopadhyay, K. (2014) Functional characterization of *Helicobacter pylori* TlyA: Pore-forming hemolytic activity and cytotoxic property of the protein. *Biochem. Biophys. Res. Commun. 444*, 153−157.

(15) Zhang, Z. W., Dorrell, N., Wren, B. W., and Farthingt, M. J. (2002) *Helicobacter pylori* adherence to gastric epithelial cells: A role for non-adhesin virulence genes. *J. Med. Microbiol. 51*, 495−502.

(16) Lata, K., and Chattopadhyay, K. (2014) *Helicobacter pylori* TlyA agglutinates liposomes and induces fusion and permeabilization of the liposome membranes. *Biochemistry 53*, 3553−3563.

(17) Conway, K. A., Harper, J. D., and Lansbury, P. T., Jr. (2000) Fibrils formed in vitro from α-synuclein and two mutant forms linked to Parkinson's disease are typical amyloid. *Biochemistry 39*, 2552−2563.

(18) Ray, A., Chattopadhyay, K., Banerjee, K. K., and Biswas, T. (2003) Macrophage distinguishes *Vibrio cholerae* hemolysin from its protease insensitive oligomer by time dependent and selective expression of CD80-CD86. *Immunol. Lett. 89*, 143−147.

(19) Schuck, P., Perugini, M. A., Gonzales, N. R., Howlett, G. J., and Schubert, D. (2002) Size-distribution analysis of proteins by analytical ultracentrifugation: Strategies and application to model systems. *Biophys. J. 82*, 1096−1111.

(20) de Groot, N. S., and Ventura, S. (2006) Effect of temperature on protein quality in bacterial inclusion bodies. *FEBS Lett. 580*, 6471−6476.

(21) Paul, K., and Chattopadhyay, K. (2012) Single point mutation in *Vibrio cholerae* cytolysin compromises the membrane pore-formation mechanism of the toxin. *FEBS J. 279*, 4039−4051.

(22) Fernandez-Escamilla, A. M., Rousseau, F., Schymkowitz, J., and Serrano, L. (2004) Prediction of sequence-dependent and mutational effects on the aggregation of peptides and proteins. *Nat. Biotechnol. 22*, 1302−1306.

(23) Linding, R., Schymkowitz, J., Rousseau, F., Diella, F., and Serrano, L. (2004) A comparative study of the relationship between protein structure and β-aggregation in globular and intrinsically disordered proteins. *J. Mol. Biol. 342*, 345−353.

(24) Rousseau, F., Schymkowitz, J., and Serrano, L. (2006) Protein aggregation and amyloidosis: Confusion of the kinds? *Curr. Opin. Struct. Biol. 16*, 118−126.

(25) Maurer-Stroh, S., Debulpaep, M., Kuemmerer, N., Lopez de la Paz, M., Martins, I. C., Reumers, J., Morris, K. L., Copland, A., Serpell, L., Serrano, L., Schymkowitz, J. W., and Rousseau, F. (2010) Exploring the sequence determinants of amyloid structure using position-specific scoring matrices. *Nat. Methods 7*, 237−242.

(26) Bolton, D. C., McKinley, M. P., and Prusiner, S. B. (1982) Identification of a protein that purifies with the scrapie prion. *Science 218*, 1309−1311.

(27) Matsuyama, S., and Taguchi, F. (2002) Receptor-induced conformational changes of murine coronavirus spike protein. *J. Virol. 76*, 11819−11826.

(28) Stryer, L. (1965) The interaction of a naphthalene dye with apomyoglobin and apohemoglobin. A fluorescent probe of non-polar binding sites. *J. Mol. Biol. 13*, 482−495.

(29) Hawe, A., Sutter, M., and Jiskoot, W. (2008) Extrinsic fluorescent dyes as tools for protein characterization. *Pharm. Res. 25*, 1487−1499.

(30) Mulqueen, P. M., and Kronman, M. J. (1982) Binding of naphthalene dyes to the N and A conformers of bovine α-lactalbumin. *Arch. Biochem. Biophys. 215*, 28−39.

(31) Engelhard, M., and Evans, P. A. (1995) Kinetics of interaction of partially folded proteins with a hydrophobic dye: Evidence that molten globule character is maximal in early folding intermediates. *Protein Sci. 4*, 1553−1562.

DOI: 10.1021/acs.biochem.5b00423
Biochemistry 2015, 54, 3649−3659

(32) Matthews, C. R. (1993) Pathways of protein folding. *Annu. Rev. Biochem. 62*, 653−683.
(33) Gabellieri, E., and Strambini, G. B. (2003) Perturbation of protein tertiary structure in frozen solutions revealed by 1-anilino-8-naphthalene sulfonate fluorescence. *Biophys. J. 85*, 3214−3220.
(34) Bismuto, E., Gratton, E., and Lamb, D. C. (2001) Dynamics of ANS binding to tuna apomyoglobin measured with fluorescence correlation spectroscopy. *Biophys. J. 81*, 3510−3521.
(35) Guha, S., and Bhattacharyya, B. (1995) A partially folded intermediate during tubulin unfolding: Its detection and spectroscopic characterization. *Biochemistry 34*, 6925−6931.
(36) Bolognesi, B., Kumita, J. R., Barros, T. P., Esbjorner, E. K., Luheshi, L. M., Crowther, D. C., Wilson, M. R., Dobson, C. M., Favrin, G., and Yerbury, J. J. (2010) ANS binding reveals common features of cytotoxic amyloid species. *ACS Chem. Biol. 5*, 735−740.
(37) Oguchi, Y., Takeda, K., Watanabe, S., Yokota, N., Miki, K., and Tokuda, H. (2008) Opening and closing of the hydrophobic cavity of LolA coupled to lipoprotein binding and release. *J. Biol. Chem. 283*, 25414−25420.
(38) Paul, K., and Chattopadhyay, K. (2011) Unfolding distinguishes the *Vibrio cholerae* cytolysin precursor from the mature form of the toxin. *Biochemistry 50*, 3936−3945.
(39) Maskevich, A. A., Stsiapura, V. I., Kuzmitsky, V. A., Kuznetsova, I. M., Povarova, O. I., Uversky, V. N., and Turoverov, K. K. (2007) Spectral properties of thioflavin T in solvents with different dielectric properties and in a fibril-incorporated form. *J. Proteome Res. 6*, 1392−1401.
(40) Biancalana, M., and Koide, S. (2010) Molecular mechanism of Thioflavin-T binding to amyloid fibrils. *Biochim. Biophys. Acta 1804*, 1405−1412.
(41) Groenning, M. (2010) Binding mode of Thioflavin T and other molecular probes in the context of amyloid fibrils: Current status. *J. Chem. Biol. 3*, 1−18.
(42) Naiki, H., Higuchi, K., Hosokawa, M., and Takeda, T. (1989) Fluorometric determination of amyloid fibrils in vitro using the fluorescent dye, thioflavin T1. *Anal. Biochem. 177*, 244−249.
(43) Sulatskaya, A. I., Kuznetsova, I. M., and Turoverov, K. K. (2011) Interaction of thioflavin T with amyloid fibrils: Stoichiometry and affinity of dye binding, absorption spectra of bound dye. *J. Phys. Chem. B 115*, 11519−11524.
(44) LeVine, H., III (1993) Thioflavine T interaction with synthetic Alzheimer's disease β-amyloid peptides: Detection of amyloid aggregation in solution. *Protein Sci. 2*, 404−410.
(45) LeVine, H., III (1999) Quantification of β-sheet amyloid fibril structures with thioflavin T. *Methods Enzymol. 309*, 274−284.
(46) Reinke, A. A., Abulwerdi, G. A., and Gestwicki, J. E. (2010) Quantifying prefibrillar amyloids in vitro by using a "thioflavin-like" spectroscopic method. *ChemBioChem 11*, 1889−1895.
(47) Ban, T., Hamada, D., Hasegawa, K., Naiki, H., and Goto, Y. (2003) Direct observation of amyloid fibril growth monitored by thioflavin T fluorescence. *J. Biol. Chem. 278*, 16462−16465.
(48) Yanagi, K., Ashizaki, M., Yagi, H., Sakurai, K., Lee, Y. H., and Goto, Y. (2011) Hexafluoroisopropanol induces amyloid fibrils of islet amyloid polypeptide by enhancing both hydrophobic and electrostatic interactions. *J. Biol. Chem. 286*, 23959−23966.
(49) Mishra, R., Sorgjerd, K., Nystrom, S., Nordigarden, A., Yu, Y. C., and Hammarstrom, P. (2007) Lysozyme amyloidogenesis is accelerated by specific nicking and fragmentation but decelerated by intact protein binding and conversion. *J. Mol. Biol. 366*, 1029−1044.
(50) Jha, S., Snell, J. M., Sheftic, S. R., Patil, S. M., Daniels, S. B., Kolling, F. W., and Alexandrescu, A. T. (2014) pH dependence of amylin fibrillization. *Biochemistry 53*, 300−310.
(51) Sackett, D. L., and Wolff, J. (1987) Nile red as a polarity-sensitive fluorescent probe of hydrophobic protein surfaces. *Anal. Biochem. 167*, 228−234.
(52) Mishra, R., Sjolander, D., and Hammarstrom, P. (2011) Spectroscopic characterization of diverse amyloid fibrils in vitro by the fluorescent dye Nile red. *Mol. BioSyst. 7*, 1232−1240.
(53) Nilsson, M. R. (2004) Techniques to study amyloid fibril formation in vitro. *Methods 34*, 151−160.
(54) Makin, O. S., and Serpell, L. C. (2005) Structures for amyloid fibrils. *FEBS J. 272*, 5950−5961.
(55) Langkilde, A. E., and Vestergaard, B. (2009) Methods for structural characterization of prefibrillar intermediates and amyloid fibrils. *FEBS Lett. 583*, 2600−2609.
(56) Goldsbury, C. S., Cooper, G. J., Goldie, K. N., Muller, S. A., Saafi, E. L., Gruijters, W. T., Misur, M. P., Engel, A., Aebi, U., and Kistler, J. (1997) Polymorphic fibrillar assembly of human amylin. *J. Struct. Biol. 119*, 17−27.
(57) Gosal, W. S., Morten, I. J., Hewitt, E. W., Smith, D. A., Thomson, N. H., and Radford, S. E. (2005) Competing pathways determine fibril morphology in the self-assembly of β2-microglobulin into amyloid. *J. Mol. Biol. 351*, 850−864.
(58) Chiti, F., and Dobson, C. M. (2006) Protein misfolding, functional amyloid, and human disease. *Annu. Rev. Biochem. 75*, 333−366.
(59) Eichner, T., Kalverda, A. P., Thompson, G. S., Homans, S. W., and Radford, S. E. (2011) Conformational conversion during amyloid formation at atomic resolution. *Mol. Cell 41*, 161−172.
(60) Eichner, T., and Radford, S. E. (2011) A diversity of assembly mechanisms of a generic amyloid fold. *Mol. Cell 43*, 8−18.
(61) Radford, S. E., and Weissman, J. S. (2012) Special issue: The molecular and cellular mechanisms of amyloidosis. *J. Mol. Biol. 421*, 139−141.
(62) Koo, E. H., Lansbury, P. T., Jr., and Kelly, J. W. (1999) Amyloid diseases: Abnormal protein aggregation in neurodegeneration. *Proc. Natl. Acad. Sci. U.S.A. 96*, 9989−9990.
(63) Muchowski, P. J. (2002) Protein misfolding, amyloid formation, and neurodegeneration: A critical role for molecular chaperones? *Neuron 35*, 9−12.
(64) Wolfe, K. J., and Cyr, D. M. (2011) Amyloid in neurodegenerative diseases: Friend or foe? *Semin. Cell Dev. Biol. 22*, 476−481.
(65) Fowler, D. M., Koulov, A. V., Alory-Jost, C., Marks, M. S., Balch, W. E., and Kelly, J. W. (2006) Functional amyloid formation within mammalian tissue. *PLoS Biol. 4*, e6.
(66) Fowler, D. M., Koulov, A. V., Balch, W. E., and Kelly, J. W. (2007) Functional amyloid: From bacteria to humans. *Trends Biochem. Sci. 32*, 217−224.
(67) Chapman, M. R., Robinson, L. S., Pinkner, J. S., Roth, R., Heuser, J., Hammar, M., Normark, S., and Hultgren, S. J. (2002) Role of *Escherichia coli* curli operons in directing amyloid fiber formation. *Science 295*, 851−855.
(68) Barnhart, M. M., and Chapman, M. R. (2006) Curli biogenesis and function. *Annu. Rev. Microbiol. 60*, 131−147.
(69) Cherny, I., Rockah, L., Levy-Nissenbaum, O., Gophna, U., Ron, E. Z., and Gazit, E. (2005) The formation of *Escherichia coli* curli amyloid fibrils is mediated by prion-like peptide repeats. *J. Mol. Biol. 352*, 245−252.
(70) Syed, A. K., and Boles, B. R. (2014) Fold modulating function: Bacterial toxins to functional amyloids. *Front. Microbiol. 5*, 401.
(71) Bavdek, A., Kostanjsek, R., Antonini, V., Lakey, J. H., Dalla Serra, M., Gilbert, R. J., and Anderluh, G. (2012) pH dependence of listeriolysin O aggregation and pore-forming ability. *FEBS J. 279*, 126−141.
(72) Romero, D., Aguilar, C., Losick, R., and Kolter, R. (2010) Amyloid fibers provide structural integrity to *Bacillus subtilis* biofilms. *Proc. Natl. Acad. Sci. U.S.A. 107*, 2230−2234.
(73) Fukui, T., Shiraki, K., Hamada, D., Hara, K., Miyata, T., Fujiwara, S., Mayanagi, K., Yanagihara, K., Iida, T., Fukusaki, E., Imanaka, T., Honda, T., and Yanagihara, I. (2005) Thermostable direct hemolysin of *Vibrio parahaemolyticus* is a bacterial reversible amyloid toxin. *Biochemistry 44*, 9825−9832.
(74) DeLano, W. L. (2002) *The PyMOL Molecular Graphics System*, DeLano Scientific, San Carlos, CA.

DOI: 10.1021/acs.biochem.5b00423
Biochemistry 2015, 54, 3649−3659